Assessment of Southwest Asia Surface Temperature Changes: CMIP5 20th and 21st Century Simulations

Babar, Z. A.[1, 2], X. Zhi[3], F. Ge[3, 4], M. Riaz[2], A. Mahmood[2], S. Sultan[2], M. A. Shad[2], C. M. Aslam[2], M. F. Ahmad[5]

Abstract

Surface temperature variability in southwest Asia during 20th century and projected changes from CMIP5 under three emission scenarios for the 21st century are assessed on the basis of a multimodel ensemble mean of 17 CMIP5 runs and two observational datasets. Performance of individual models is also compared against the observations. CMIP5 models show seasonality in biases over southwest Asia. Cold biases over the Himalayan range are more obvious in winter than in summer. The observed climatic warming during the 20th century is very well captured by the CMIP5 models. However, there is a limited agreement between the observations and the CMIP5 models ensemble mean regarding the temperature trends and their spatial distribution over southwest Asia. Surface temperature variability over southwest Asia is best represented by three individual models (BCC, HadGEM and NorESM). Temperature projections for the 21st century demonstrate that annual temperature rise for RCP 8.5 and RCP 4.5 scenarios is 0.55 °C (10 year)$^{-1}$ and 0.27 °C(10 year)$^{-1}$. The RCP 2.6 scenario has the lowest warming rate at 0.11 °C (10 year)$^{-1}$. By the end of the 21st century, the annual mean temperature in southwest Asia is estimated to increase by 0.80 °C to 4.85 °C. This warming is projected to take place mostly around Pakistan and its surrounding areas.

Key Words: CMIP5, Southwest Asia, Temperature, Variability, Pakistan

Introduction

Studies into the global observational surface temperature records show an increase in the observed temperature mean (Trenberth et al. 2007). Climate models are also able to successfully simulate these observed warming trends during the 20thcentury (Stott et al. 1998). These demonstrate that warming during the first half of the 20th century was caused by natural variation; whereas, warming during the second half of the century warming was caused by an increase in anthropogenic greenhouse gas emissions (IPCC 2001). Most of the warming that occurred in the mid-20th century took place in higher latitudes (Johannessen et al. 2004; Overland et al. 2004; Serreze & Francis 2006); whereas, warming in the latter stages of the 20th century occurred at all latitudes (Stott et al. 2000). It is well documented that the three decades from 1983 to 2012 were the warmest thirty years of the last 1400 years and also that in the period from 1880 to 2012 all land and ocean surfaces warmed by approximately 0.85 °C (IPCC 2013). Previously, it was stated by the IPCC that the global average trend of the surface temperature was a 0.7 °C rise during the 20th century (IPCC 2001; IPCC 2007). It was also observed that surface temperature, when averaged over the global scale, shows a great deal of decadal and interannual variability(IPCC 2013). Over approximately the last three decades, surface air temperature in central Asia has increased by 0.36–0.42 °C. Interestingly, unlike most parts of the world, winter temperatures in central Asia do not show the increasing trend and the increase in temperature was instead observed in spring temperatures (Hu et al. 2014). Kumar et al. (2013) found that the rate of warming in parts of north and central Asia is double than that of the global average warming.

A major portion of southwest Asia is composed of the countries of the Indian subcontinent. This includes three major countries; Pakistan, India and Bangladesh. These areas are home to 45 % of Asia's population

[1] zaheer_a_babar@hotmail.com
[2] Pakistan Meteorological Department, Flood Forecasting Division,46 Jail Road, Lahore, Pakistan.
[3] Collaborative Innovation Center on Forecast and Evaluation of Meteorological Disasters/KLME, Nanjing University of Information Science and Technology, Nanjing 210044, China.
[4] Plateau Atmosphere and Environment Key Laboratory of Sichuan Province, College of Atmospheric Sciences, Chengdu University of Information Technology, Chengdu 610225, China.
[5] Pakistan Meteorological Department, Regional Meteorological Center, Khyber Road, Peshawar, Pakistan.

or about 25 % of world population. Any change in weather patterns is likely to have a profound effect on this socially and economically vulnerable area. On a regional basis; Bangladesh from 1985 to 1998 recorded an increasing trend of about 1 °C in May and 0.5 °C in November. India reported a 0.68 °C rise per century and the warming was more pronounced in winter. Nepal reported a 0.09 °C per year increase in the Himalaya region. Coastal areas of Pakistan recorded a 0.6–1.0 °C increase in the mean temperature since early 1900 (Cruz et al. 2007). For India a considerable warming trend of 0.57 °C (100 year)$^{-1}$ was found by Pant & Kumar (1997). A latter study also showed that mean temperature over India shows an increase of 0.42 °C (100 year)−1;however, seasonal analyses reveal no significant trend in the monsoon and pre-monsoon temperatures (Arora et al. 2005). A slight warming trend, with no significant trend in precipitation was observed for India by Sarker & Thapliyal (1988). It has also been observed that diurnal temperature trends over India are quite different to those found in different parts of the world (Srivastava et al. 1992). In the case of Pakistan, studies show that different parts of country may experience changing climatic patterns, thus affecting various aspects of life (Farooqi et al. 2005). Uncertainties in weather patterns caused by climate change may disrupt the normal patterns of onset and withdrawal of monsoon. It may also alter the number of rainfall days and frequency of extreme weather events (Imran et al. 2014).

It has been suggested that annual mean maximum and annual mean minimum surface air temperatures over India in the 2040s would vary from about 0.7 °C to 1.0 °C compared with the temperatures in the 1980s (Lal et al. 2001). The output from different General Circulation Models (GCMs) varies considerably and the average change across India is said to be likely to be in the range of 2.3 °C to 4.8 °C (Arora et al. 2005). The Coupled Model Inter-comparison Project phase five (CMIP5) is a suite of climate model outputs called the CMIP series. CMIP outputs are produced by world leading climate modeling groups. These simulations are of international importance and contribute strongly to the Intergovernmental Panel on Climate Change Fifth Assessment Report (AR5). CMIP5 model outputs are expected to improve the prediction and knowledge of future climate change (Taylor et al. 2012). It has been noted that most of the CMIP5 models tend to produce a cooler than observed global mean temperature during the twentieth century and the observed trend is overestimated in their hindcasts (Kim et al. 2012).

This study is intended to investigate the surface temperature changes during the 20th and 21st century in southwest Asia. Temperature change analyses during the 20th century were performed using three different surface air temperature datasets to minimize the impact of the choice of the dataset on the results. The results from these different datasets are also compared using the ensemble mean of a historical CMIP5 model experiment. Projected changes in temperature during the 21st century are examined not only from the individual models but also by the ensemble mean obtained from the CMIP5 models for the three Representative Concentration Pathways (RCP) scenarios (RCP 2.6, RCP 4.5 and RCP 8.5).

The paper is structured as follows: datasets and methods used in the analysis are discussed in Section 2. Temperature changes during the 20th century are explained in Section 3. The fourth section gives the projected temperature changes during the 21st century by considering the three RCP scenarios. Concluding remarks are presented in Section 5.

Data and Methods

CMIP5 Models

This study used model outputs from 17 GCMs of the CMIP5 model suite. Details of these models and their respective modeling centers are given in Table 1. This work utilizes four sets of experiments from CMIP5 model outputs, historical experiments for the 20th century and RCPs (RCP 2.6, RCP 4.5 and RCP 8.5). The simulations for historical experiment are from 1850–2005. These are based on observed natural and anthropogenic forcings. Future climate projections for different emission scenarios are based on the period 2006–2300. However, the present modelling effort was based on climate projections from 2006–2100. This work also does not use the RCP 6.0 scenario. The RCPs adopted by IPCC AR5 essentially represent different radiative forcings. RCP 2.6 is known as the low emission scenario; its radiative forcing reaches a value of about 3.1 W/m^2 in the mid-century, returning to 2.6

W/m^2 by 2100 (Van Vuuren et al. 2007). RCP4.5 is a medium stabilization scenario where total radiative forcing is stabilized before 2100 (Clarke et al. 2007; Wise et al. 2009). RCP6.0 is also a stabilization scenario where total radiative forcing is stabilized after 2100 (Fujino et al. 2006; Hijioka et al. 2008). RCP 8.5 is characterized by increasing greenhouse gas emission; the scenario is based on high population growth and high energy demand without considering climate change mitigation policies, thus leading to high greenhouse gas concentrations (Riahi et al. 2007).

Domain of the Study

The area covered in this study is between 5°N to 45°N and from 45°E to 95°E. This comprises of Pakistan, India, Bangladesh, Nepal, Iran, Afghanistan and parts of Saudi Arabia and Oman

Observed Data

Three surface air temperature datasets were used to evaluate the performance of the CMIP5 models. One is the Climate Research Unit (CRU) time-series (TS) 3.21 mean temperature dataset from the University of East Anglia; this is the global land surface dataset at 0.5°×0.5° resolution for the period 1901–2012 (Harris et al. 2014). The second observational dataset is from the University of Delaware (UDEL) and also provides mean temperature land surface data but at 1°×1° resolution for the period 1900–2009 (Willmott & Robeson 1995). The third observational dataset is NASA GISS Surface Temperature (GISTEMP) anomaly dataset from 1880–2013, where anomalies are relative to the 1951–1980 base period (Hansen et al. 2006). These data are at 2°×2° resolution from 1880–2013. For relative study of temperature during the 20thcentury CRU and UDEL were used because they both are spatially and temporally comprehensive from 1901 onward.

Table 1: Name of the modeling centers, institute ID, model name, and horizontal resolution for models included in the CMIP5 model suite**.**

Modeling Center	Model Name	Horizontal Resolution
Commonwealth Scientific and Industrial Research Organization (CSIRO) and Bureau of Meteorology (BOM), Australia	ACCESS1.0	~1.8°× 1.25°
Beijing Climate Center	BCC-CSM1.1	~2.8°× 2.8°
College of Global Change and Earth System Science, Beijing Normal University	BNU-ESM	~2.8°× 2.8°
Commonwealth Scientific and Industrial Research Organization	CSIRO-Mk3.6.0	~1.8°×1.8°
Canadian Centre for Climate Modelling and Analysis	CanESM2	~2.8°× 2.8°
National Center for Atmospheric Research	CCSM4	~0.9°× 1.5°
EC-EARTH consortium	EC-EARTH	~1.1°× 1.1°
LASG, Institute of Atmospheric Physics, Chinese Academy of Sciences and CESS, Tsinghua University	FGOALS-g2	~1.6°× 2.8°
Met Office Hadley Centre (additional HadGEM2-ES realizations contributed by InstitutoNacional de PesquisasEspaciais)	HadCM3	~3.7°× 2.5°
Met Office Hadley Centre (additional HadGEM2-ES realizations contributed by InstitutoNacional de PesquisasEspaciais)	HadGEM2-CC	~1.2°× 1.8°
Atmosphere and Ocean Research Institute, The University of Tokyo	MIROC5	~1.4°× 1.4°

NASA Goddard Institute for Space Studies	GISS-E2-H-CC	~2°×2.5°
Institute for Numerical Mathematics, Russia	INM-CM4	~1.5°×2°
Institut Pierre-Simon Laplace	IPSL-CM5A-LR	~4.1°×3.7°
Max Planck Institute for Meteorology	MPI-ESM-LR	~1.8°×1.8°
Meteorological Research Institute	MRI-CGCM3	~1.1°×1.1°
Norwegian Climate Centre	NorESM1-M	~1.8° × 2.5°

Methods

For temperature analysis bilinear interpolation was used to normalize all CMIP5 outputs from 17 models into an identical resolution of 2.5°×2.5°. Some modeling groups have used multiple realization schemes for each experiment; however, in this work a single realization scheme (r1i1p1) was used. These outputs were then used to create a multimodel ensemble mean of CMIP5. During the period 1901–2005 data from the historical simulations was used and for the period 2006–2100 data from three RCP experiments, RCP 2.5, RCP 4.5 and RCP 8.5, was utilized. For detailed examination, the 20th century was divided into two periods, 1901–1949, and 1950–1999. Monthly, seasonal and annual temperatures trends were calculated using linear trend analyses in the domain of 5–45 °N and 45–95 °E, an area mainly covered by southwest Asia. This was performed for both the 20th and 21st centuries. Individual CMIP5 model outputs were also compared and evaluated using various statistical techniques.

Temperature in the 20th Century

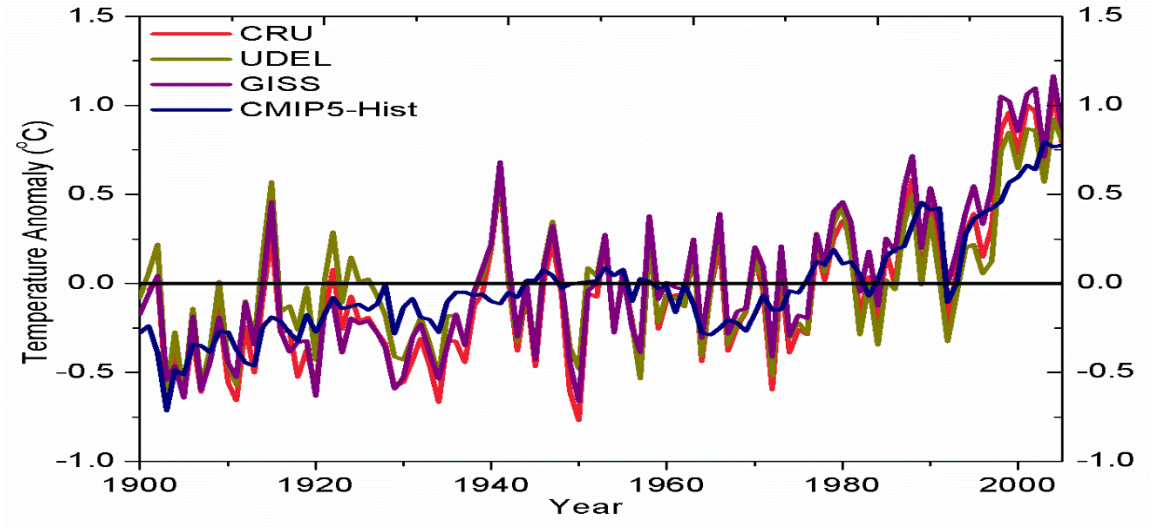

Figure 1: Time series of temperature anomaly extracted from the CRU, UDEL, GISS and CMIP5 multimodel ensemble mean.

Annual temperature anomalies during the 20th century are presented in Figure 1. These are from the three observational datasets and the multimodel ensemble mean of the CMIP5 historical experiments (CMIP5-Hist). Anomalies are taken by considering 1961–1990 as the baseline. All the three observational datasets seem to be in good agreement with each other and this agreement improves further during the second half of the century. Observational discrepancies during the first half of the century may be because of the limited number of observatories and instrumental disparity. The correlation during the period of 1901–2000

between CRU–UDEL and CRU–GISS is 0.95 and 0.98, respectively. The correlation between UDEL and GISS is 0.91. All the datasets show an improved correlation during 1951–2000. Correlation between CRU–UDEL and CRU–GISS becomes 0.97 and 0.99, respectively, and between UDEL–GISS is 0.95. During the first half of the century, datasets, show a slight in consistency regarding the magnitude of peaks and troughs of the temperature time series. However, all three datasets show two very distinct peaks of temperatures, one around the 1910s and the other is around the 1940s. The dip in temperature around the 1950s is also well captured by the datasets. During the latter half of the century the observational datasets are well in phase.

The CMIP5 simulations show an overall warming trend throughout the 20th century. This trend is quite visible after the 1980s. As CMIP5 is the ensemble mean of all the model outputs, it is not able to reproduce the highs and lows of the temperature anomaly. During the first half of the century, CMIP5 generally captures the cooling trend of the temperature. In the period around the 1930s CMIP5 models show warmer temperatures than the observed datasets. CMIP5 is also not able to capture the peaks of 1910 and the 1940s and the trough of the 1950s. However, the dip in temperature during the 1990s is well captured by the CMIP5 ensemble mean. CMIP5 shows comparatively less warming than the three observational datasets by the end of the 20th century.

Table 2: Annual and seasonal temperature means and trends, during the 20th century, for the region obtained from UDEL and CRU observations and CMIP5 multimodel ensemble. For correlation, the bold values are significant at the 95 % level.

	Annual	Summer	Winter
	Mean Temperature (°C)		
CRU	16.42	24.52	7.03
UDEL	16.35	24.54	6.82
CMIP5	15.15	24.41	4.93
	Temperature Difference (°C)		
CRU–UDEL	0.070	−0.016	0.209
CMIP5–CRU	−1.278	−0.107	−2.100
CMIP5–UDEL	−1.208	−0.123	−1.891
	Pearson Correlation		
CRU and UDEL	**0.95**	**0.93**	**0.97**
CMIP5 and CRU	**0.68**	**0.62**	**0.35**
CMIP5 and UDEL	**0.57**	**0.53**	**0.27**
	1901–2000 Trend (°C(100year)$^{-1}$)		
CRU	0.77	0.56	1.78
UDEL	0.58	0.57	0.80
CMIP5	0.84	0.77	0.84

Table 2 shows the annual and seasonal temperature means and trends of the region obtained from UDEL and CRU observations and CMIP5 multimodel ensemble mean. Mean annual temperature of CMIP5 is less than as compared to simulated by both CRU and UDEL. These cold biases also exist in the mean summer and winter temperatures. High correlation exists between the mean annual observational datasets and the CMIP5 ensemble mean. Correlation of CMIP5 with CRU and UDEL is 0.68 and 0.57, respectively. This implies that CMIP5 multimodel ensemble mean captures 32–46 % of observational temperature variability.

Correlation is significantly weak between the mean winter temperatures compared with the mean summer temperatures.

Results in table 2 show that there are prominent warming trends in annual temperatures during the 20th century. The CRU data have the largest warming rate of 0.77 °C (100 year)$^{-1}$ for the region. This is quite similar to the global temperature increase. The UDEL data indicate a trend of 0.58 °C (100 year)$^{-1}$. In contrast, the CMIP5 data show a warming trend of 0.84 °C (100 year)$^{-1}$. Seasonal analyses of the observational datasets indicate that most of the warming has taken place in the winter season. This implies that warming over southwest Asia is driven by the considerable warming trend in the winter season. CMIP5 does not show any significant seasonal variability. However, it does show a stronger warming trend in winter than in summer. In CMIP5, the rate of increase of temperature during winter is very much lower than that derived from CRU but is nearly same to that of UDEL.

Table 3 give the temperature biases and trends during the first and second halves of the 20th century, respectively. This gives a comparative look of the two halves of the last century. The data during the second half of the century are more reliable, owing to an improved network of observational stations and better data quality control and instrumental efficiency. Both the observational datasets show a slightly higher mean annual temperature during the second half of the century compared with the first half. This difference is also seen in the seasonal temperatures. Winter mean temperature shows a greater temperature rise than in summer. Correlation between the two observational datasets also improves in the second half of the century. This improvement of correlation during the second half of the century is also seen between CMIP5–CRU and CMIP5–UDEL. The CRU datasets also indicate the largest warming of 0.2 °C (10 year)$^{-1}$ during the second half of the century.

Table 3: Annual and seasonal temperature means and trends, during 1951–2000 for the region obtained from UDEL and CRU observations and CMIP5 multimodel ensemble. For correlation, the bold values are significant at the 95 % level.

	Annual	Summer	Winter
	Mean Temperature (°C)		
CRU	16.54	24.59	7.26
UDEL	16.40	24.55	6.94
CMIP5	15.24	24.50	5.03
	Temperature Difference (°C)		
CRU–UDEL	0.14	0.04	0.32
CMIP5–CRU	−1.30	−0.09	−2.23
CMIP5–UDEL	−1.16	−0.06	−1.91
	Pearson Correlation (1951–2000)		
CRU and UDEL	**0.97**	**0.97**	**0.97**
CMIP5 and CRU	**0.71**	**0.67**	**0.41**
CMIP5 and UDEL	**0.62**	**0.64**	**0.33**
	1951–2000 Trend (°C (10 year)$^{-1}$)		
CRU	0.13	0.09	0.21
UDEL	0.07	0.06	0.11
CMIP5	0.09	0.09	0.10

Table 4 exhibits a series of statistical analyses that were performed on CMIP5 model outputs for June–July–August (JJA) mean surface temperatures. This was performed to identify the models that are best suited to simulate the summer temperature variability over the region. Multimodel ensemble mean is also calculated for these outputs as it is expected to reduce the forecast noise. In this case CMIP5 models show a large amount of variability between its component models. Many models show a high correlation with the observations and smaller errors as compared to the observational datasets. INM-CM, IPSL, BCC and EC-Earth all show a high correlation with the observational dataset, similarly BCC, NorESM, GISS have a small root mean square error(RMSE). FGOALS, GISS, ACCESS and MRI have a small standard deviation. EC-Earth and INM-CM have the largest cold biases and MIROC5 has the largest warm bias.

Table 4: Evaluation of individual CMIP5 model outputs for June–July–August (JJA) temperatures relative to CRU (JJA) temperatures based on Pearson correlation coefficient (R), mean error (ME), mean absolute error (MAE), standard deviation (Stdev) and root mean square error (RMSE). Values significant at the 95 % level are indicated in bold.

	R	ME (°C)	MAE (°C)	Stdev (°C)	RMSE (°C)	Trend (°C(100 yr)$^{-1}$)
CMIP5	**0.62**	−0.11	0.11	0.23	0.24	**0.77**
ACCESS	**0.21**	−0.54	0.54	0.27	0.64	0.22
BCC	**0.54**	−0.05	0.05	0.38	0.33	**0.88**
BNU	**0.41**	1.25	1.25	0.51	1.33	**0.48**
CanESM	**0.36**	1.77	1.77	0.48	1.83	**1.35**
CCSM	**0.50**	0.26	0.26	0.45	0.47	**1.45**
CSIRO	0.18	1.21	1.21	0.34	1.27	0.76
EC-Earth	**0.52**	−2.49	2.49	0.42	2.52	**0.95**
FGOALS	-0.06	−1.26	1.26	0.22	1.31	**0.12**
GISS	**0.33**	−0.22	0.22	0.27	0.38	**0.78**
HadCM	**0.32**	−0.40	0.40	0.35	0.54	**0.27**
HadGEM	**0.53**	0.99	0.99	0.37	1.04	**0.90**
INM-CM	**0.58**	−2.84	2.84	0.41	2.86	**0.86**
IPSL	**0.56**	−1.59	1.59	0.42	1.62	**1.72**
MIROC5	**0.29**	2.09	2.09	0.35	2.13	**0.78**
MPI	**0.50**	0.57	0.57	0.40	0.67	**1.30**
MRI	**0.34**	1.01	1.01	0.32	1.06	**0.65**
NorESM	**0.52**	−0.17	0.17	0.37	0.37	**0.89**

A Taylor diagram (Taylor 2001) was drawn to provide a graphical summery of the CMIP5 model outputs for surface temperature during the JJA summer months in the 20th century and their comparison with CRU data. The Taylor diagram is used to compute the similarity among the models in terms of their correlation, RMSE and standard deviation. This diagram is particularly useful to comprehend the relative proficiency of different models. Figure 2 shows the Taylor diagram for 17 CMIP5 model outputs for the mean JJA surface air temperature. It is evident from this figure that the ensemble mean of the CMIP5 model output is better than any of the individual models in terms of better correlation and lower standard deviation. INM-CM has the highest correlation coefficient, closely followed by IPSL. HadGEM, BCC and NorESM seem to have a similar relative skill. ACCESS, CSIRO and FGOALS are not able to perform very well. INM-CM and IPSL both have a high correlation, but these two models also have a high cold bias. Therefore,

HadGEM, BCC and NorESM may be considered better than others to represent temperature variability over southwest Asia on an individual model basis.

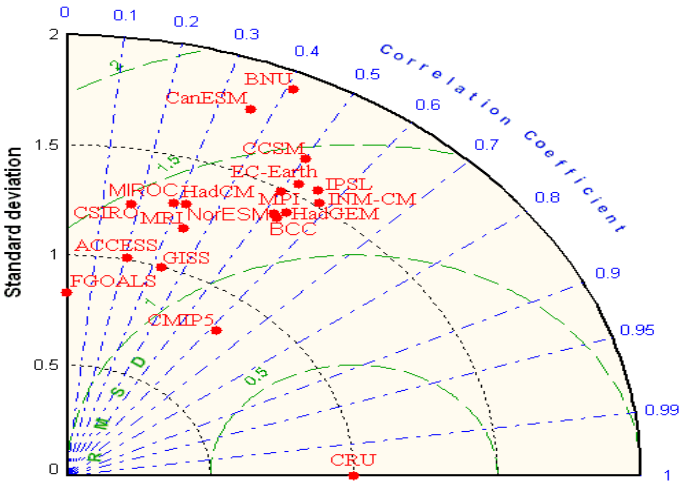

Figure 2: Taylor Diagram showing the statistical comparison of 17 CMIP5 model outputs for JJA surface air temperature with CRU surface air temperature data.

The spatial variability of annual mean temperature over southwest Asia was determined by calculating the bias in CMIP5 models as compared to CRU observations. Figure 3(a) presents the difference between mean annual temperatures derived from the CMIP5 multimodel ensemble mean and the CRU observational dataset. The CMIP5 ensemble mean shows a cold bias over the Himalayan range and the Tibetan Plateau, located north of the Indian subcontinent. The plain areas of Indian peninsula show a little cold bias. Figures 3(b) and 3(c) present the summer and winter biases in CMIP5 datasets with respect to CRU. These figures show seasonality in temperature bias in southwest Asia. This seasonality is quite evident in the plain areas of Indian peninsula where in summer most areas show a warm bias, but in winter this reverts to a cold bias. Most parts of Iran and adjoining areas of Afghanistan also show a warm bias in summer and cold bias in winter. In the case of Pakistan, the cold bias is more significant in winter than in summer. The cold bias over the Himalayan range and Tibetan Plateau can be seen in both the seasons but it is more prominent in the winter season. During the summer season, a very prominent warm bias is also present in Central Asian States. Cold biases over the mountainous north indicate the inability of CMIP5 models to simulate well over complex terrains.

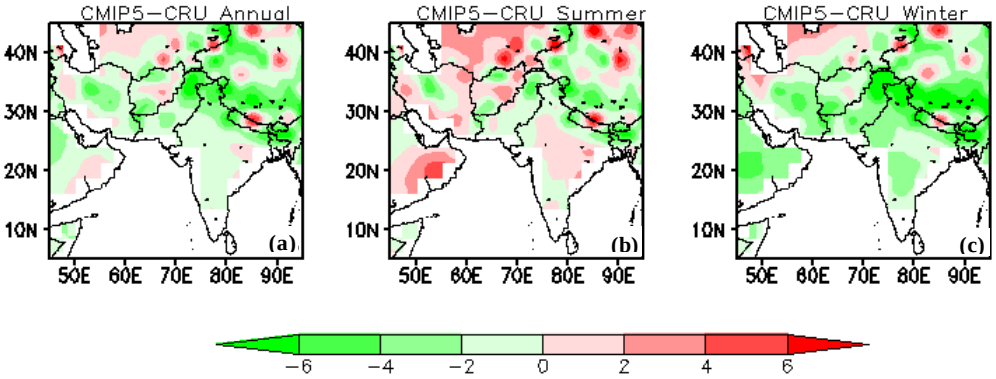

Figure 3: Annual and seasonal temperature biases of CMIP5 relative to CRU for **(a)** annual, **(b)** summer and **(c)** winter data. Green shades indicate negative while red shades indicate positive biases.

Figure 4 demonstrates the annual spatial trends during the 20th century over the region. Both CRU and UDEL show the largest warming trends over parts of Afghanistan and adjoining areas of Iran. This warming trend is also evident over areas of southwestern and extreme northern parts of Pakistan. However, UDEL

does not show any particular warming trend over India. CRU demonstrates a warming trend over eastern parts of India. This dataset also shows a warming trend over eastern and central parts of Arabian Peninsula, but this warming is not significantly shown by UDEL. Compared with these datasets, CMIP5 overestimates the warming trend in most parts of the region. CMIP5 is not able to reproduce the spatial pattern of the warming trend during the 20th century. Temperature trends show a declining tendency in central and southern parts of India, but this cooling is not very well captured by CMIP5 multimodel ensemble mean.

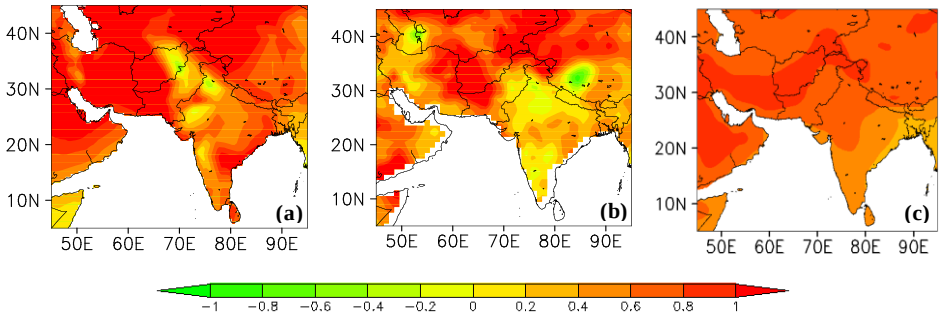

Figure 4: Trends in annual temperatures during the 20th century as obtained from **(a)** CRU, **(b)** UDEL and **(c)** CMIP5 datasets. Green shades show negative trends while positive trends are indicated by red shades

Figure 5 shows seasonal variability in temperature trends during the 20th century. This was evaluated by calculating the monthly trends from the two observational datasets CRU and UDEL and from individual model outputs of CMIP5, along with the multi model ensemble mean of the CMIP5 outputs. Both the observational datasets show a warming trend throughout the year, with the exception of March and November which have a cooling trend. Between the two observational datasets, CRU has a greater warming trend in the months of January, February, March, November and December. No clear seasonality is shown in the temperature trends during the 20th century; however, more warming is evident in the winter months than the summer months. The CMIP5 ensemble mean is the average of all the model outputs and is not able to capture any of the temperature variations. The majority of the individual models show a warming trend in most of the months during the year. The cooling trend in March is captured by four of the models (BNU, FGOALS, MRI and NorESM); whereas, cooling in November is shown by three models (CESM, GISS and MIROC). The largest warming trend is shown by MIROC and IPSL in January and December, respectively, while the largest cooling is shown by MRI in October.

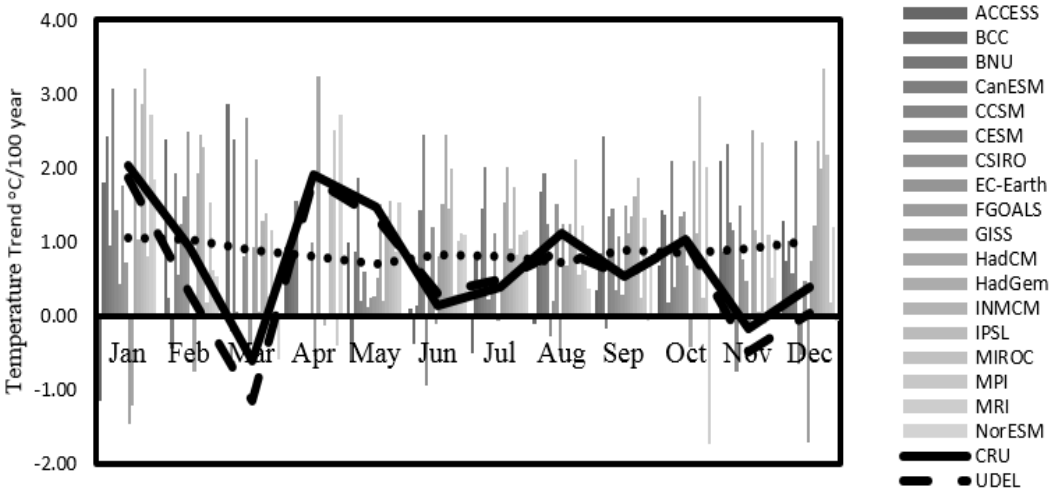

Figure 5: Trends in seasonal temperatures during the 20th century obtained from the CMIP5 model outputs, their ensemble mean and the two observational datasets, CRU and UDEL.

Temperature in the 21st Century

Projected temperature changes for southwest Asia are shown in Figure 6. Between the three emission scenarios, RCP 8.5 shows the highest rate 0.55 °C (10 year)$^{-1}$ temperature increase for mean annual temperature during the 21stcentury, followed by RCP 4.5 and RCP 2.6 at 0.27 °C (10 year)$^{-1}$ and 0.11 °C (10 year)$^{-1}$, respectively. By the end of 21st century the temperature over southwest Asia is projected to increase by 0.80–4.85 °C (Table 6). The three RCP scenarios are very close to each other till 2030s after that they become significantly different. Under the RCP 2.6 scenario, temperature increase during 2000 to 2025 is larger than the temperature rise under RCP 4.5 and RCP 8.5 scenarios, becoming stable around the 2030s. By the end of the century a slight decrease in the temperature is apparent, this is expected to be because of climate mitigation efforts, in terms of radiative forcing embedded in the structure of RCP 2.6. The temperature increase during the initial years for RCP 2.6 is greater than for the other two scenarios, though its radiative forcing is less than both RCP 4.5 and RCP 8.5. For seasonal analyses, the winter season shows a greater warming trend than the summer; it ranges from 0.12 °C (10 year)$^{-1}$ to 0.58 °C (10 year)$^{-1}$. During summer it is from 0.11 °C (10 year)$^{-1}$ to 0.53 °C (10 year)$^{-1}$. Temperature change by the end of the 21st century during the winter season is clearer than in the summer season. Temperature change in winter is in the range of 0.84–4.80 °C and in summer it is 0.79–4.71 °C (Table 5).

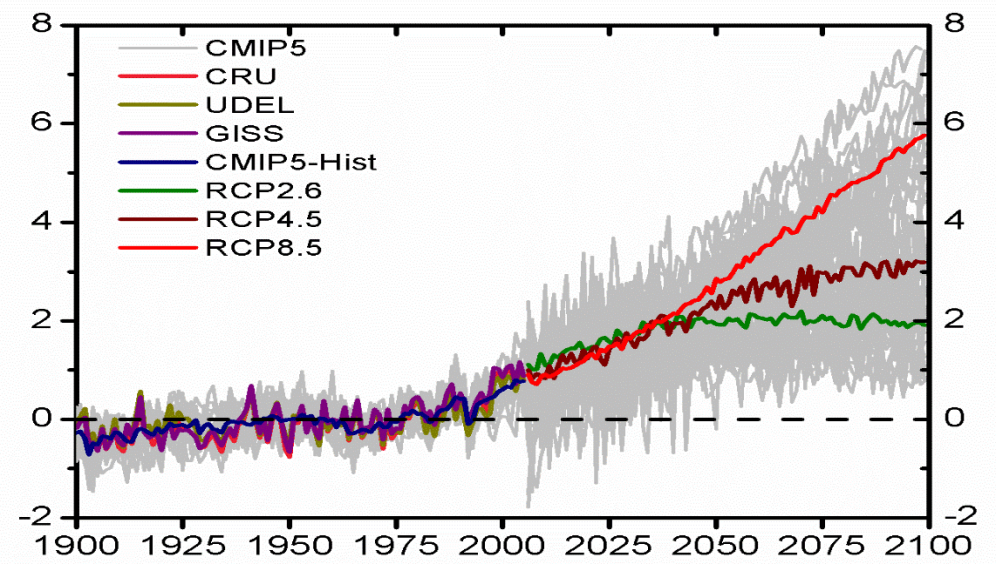

Figure 6: Time series of historical and projected temperatures for southwest Asia derived from three CMIP5 experiments.

Table 5: Projected warming in southwest Asia during the 21st century.

Experiments	Temperature Trend (°C(10 year)$^{-1}$)			Temperature Change (°C)		
	Annual	Summer	Winter	Annual	Summer	Winter
RCP2.6	0.11	0.11	0.12	0.80	0.79	0.84
RCP4.5	0.27	0.26	0.28	2.10	2.12	2.19
RCP8.5	0.55	0.53	0.58	4.85	4.71	4.80

Figure 7 shows the spatial patterns of annual and seasonal temperature changes under the three emission scenarios. These were calculated as the temperature difference between 2070–2099 and 1971–2000. Prominent higher temperatures are found in the last three decades of 21st century compared with the last three decades of the 20th century. Most of the warming takes place over Pakistan and its adjoining areas. This warming is more prominent in the winter season in the RCP 8.5 scenario. Most parts of India show

considerably less warming. This warming is also present over parts of Iran, Afghanistan and eastern parts of Saudi Arabia. Again the winters of 21st century are seen having the higher temperatures as compared to the winters of 20th century. Summers are also seen to be warmer in the 21st century than in the previous century. Summer warming is less compared to the winter warming.

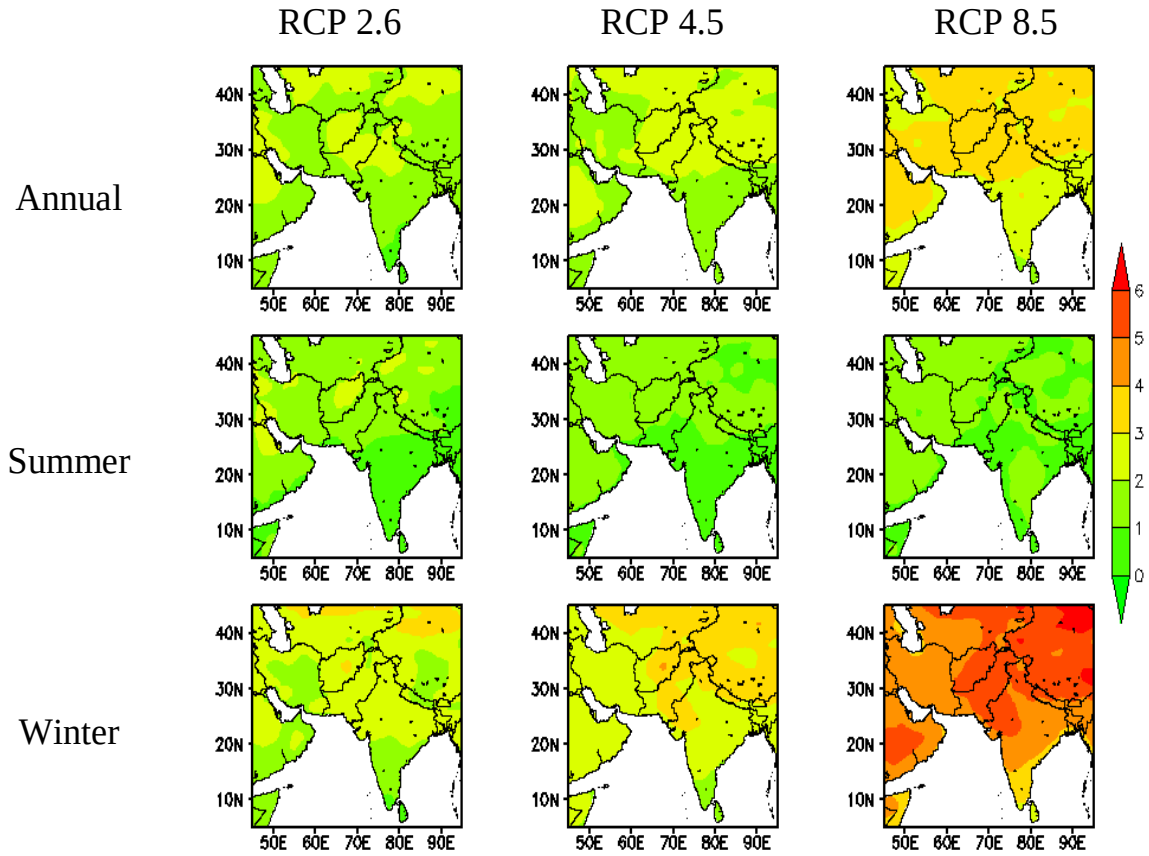

Figure 7: Annual and seasonal temperature changes (°C) in the 21st century for the three projection experiments based on CMIP5 multi model ensemble mean.

Figure 8 represents annual and seasonal trends during the 21st century, which were obtained from individual CMIP5 models and the multi model ensemble mean of all these models. For RCP 4.5 and RCP 8.5 all the models show a warming trend during the 21st century at the annual as well as the two seasonal scales. Cooling trends are only found in RCP 2.6. CCSM shows a cooling trend in the annual and both seasonal scales. FGOALS, MPI and MRI show cooling trends only in the winter season. The largest cooling trend in winter is shown by MPI. For the annual scale and during winter season, the largest warming trend is given by ACCESS. During the summer season the largest warming trend is shown by CSIRO. All the largest warming trends are exhibited in RCP 8.5 scenario. Because of the large intra-model variability it would be very difficult to identify the expected temperature trend during the 21st century. A few models show greater warming in the summer season while most show it in the winter season. RCP 2.6 BNU, CanESM and IPSL show a larger warming trend in summer than in the winter season. RCP 4.5 BCC, CSIRO, MIROC and MPI show a larger warming trend in summer than in winter. RCP 8.5 CanESM, CCSM, CSIRO, FGOALS, IPSL, MIROC and MPI show a more warming trend in summer than in winter. CanESM and IPSL show a greater warming trend during summer than in winter for the RCP 2.6 and RCP 8.5 scenarios. CSIRO, MIROC and MPI also show a greater warming trend in summer than in winter for the RCP 4.5 and RCP 8.5 scenarios. None of the models show more warming trends in summer than in winter for all the three RCP scenarios. Some models show almost the same warming trend for the two

seasons and the annual scale. For example, RCP 4.5 EC-Earth and MIROC have the same warming trend while there is a marked difference in the case of BNU and CCSM.

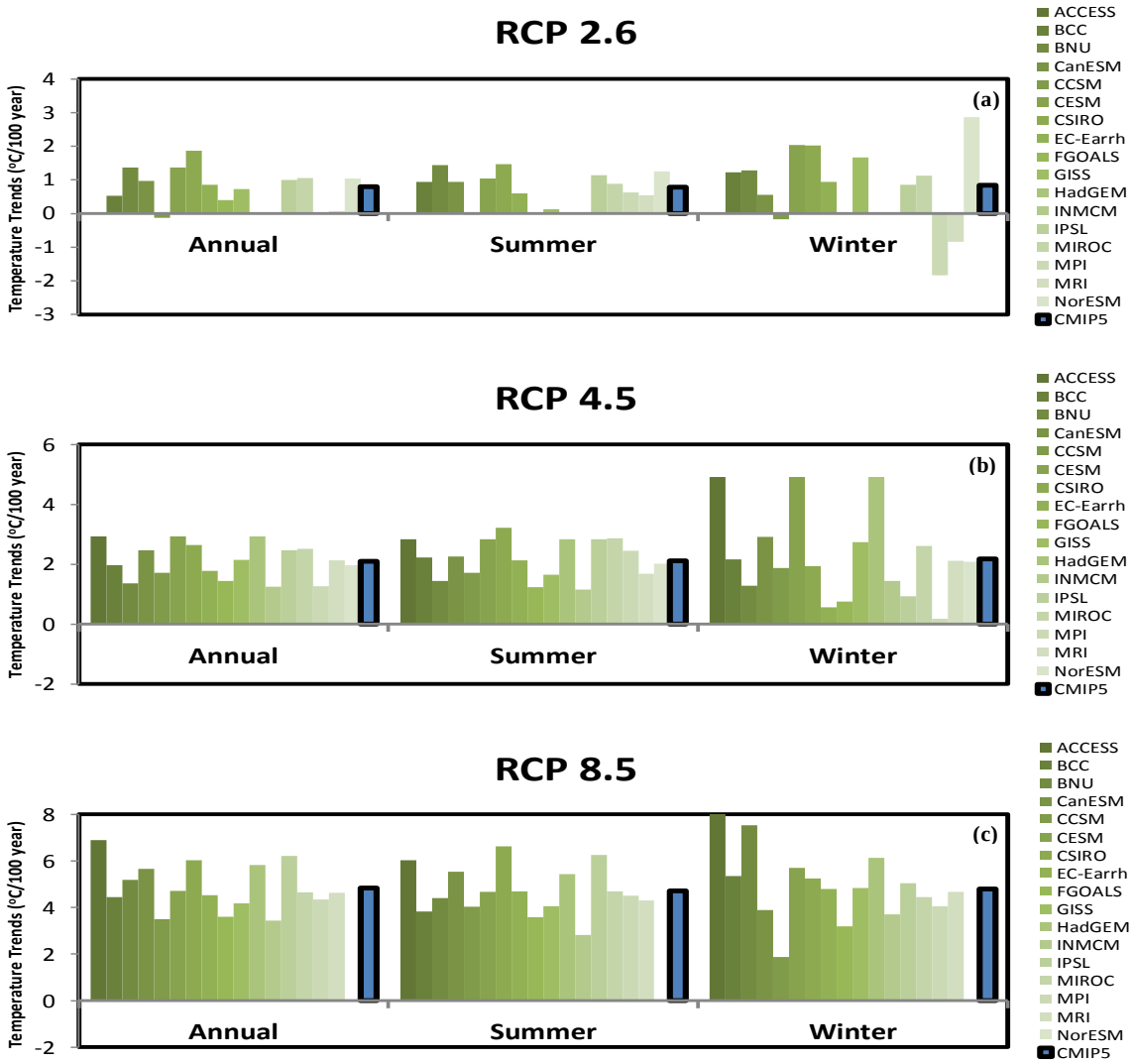

Figure 8: Annual and seasonal trends during the 21st century obtained from individual CMIP5 models and their multimodel mean (given as CMIP5) for a) RCP 2.6 b) RCP 4.5 and c) RCP 8.5

Concluding Remarks

During the 20th century CRU shows more warming than UDEL on the annual scale and during the winter season. During summer the warming rate between the two observational datasets is quite similar. The variation in warming trends may be due to the different interpolation schemes used by the two dataset centers and the observational disparities. Previous studies (e.g. Sarker & Thapliyal 1988; Pant & Kumar 1997; Arora et al. 2005) showed a warming trend over India. This is quite similar to the results obtained in this work. CMIP5 shows a greater warming trend than both CRU and UDEL. When annual and winter temperatures are considered, CMIP5 models show a considerable bias in most of the area of Indian subcontinent. For the summer season, central parts of the Indian subcontinent show a warm bias. Hence seasonality exists in the biases. No seasonality of bias is found for Pakistan. Most parts of Pakistan show a cold bias for annual and two seasonal time scales. In the case of Pakistan, a consistent cold bias can be seen in most parts of the country for mean annual and mean seasonal temperatures. Significant cold biases are

also seen over the Tibetan Plateau. These biases have a distinct seasonality; showing that cold bias is more significant in the winter season than in the summer season. These cold biases over the plateau may be due to the fact that models are not able to reproduce cloud properties, thus producing temperature biases over the Tibetan Plateau(Zhou & Li 2002; Yu et al. 2004). Northern parts of Pakistan have two large mountain ranges; therefore, the cold bias in this region may be related to the Tibetan Plateau because the Tibetan Plateau represents an elevated heat source, which may cause the models to misrepresent the snow-albedo mechanism over the region. Coarser resolution of much of the CMIP5 models may be one of the reasons for their inability to reproduce well the temperature profile over this complex region.

Simulated variability and trends from individual CMIP5 models may be inconsistent with those obtained from observational datasets. This disagreement between modeled and observed trends may be due to the limitations of the models in terms of internal variability and the different response to forcings in the models. Varying model resolutions may also be one of the factors contributing to the differences between observed and simulated datasets. It has been noted by Wu & Karoly (2007) and Wu (2010) that the changes in the leading climate variability mode, e.g. the Arctic Oscillation, can cause the discrepancy between the observations and model simulations. Wu & Straus (2004) also noted that observed surface air temperature warming over Asia can be explained through the equal contributions from the Arctic Oscillation and cold ocean–warm land patterns defined by the leading modes of an empirical orthogonal function analysis of sea level pressure. It has also been emphasized that the uncertainties in the assessment of present temperature changes may be because of the insufficient spatial coverage of observation stations and flawed methods of retrieving spatially distributed climatic variables(Karl et al. 1994; Jones & Wigley 2010). Local warming caused by urban areas may also be one of the factors influencing the spatial distribution of temperature trends(Hansen et al. 2007).

Future temperature projections show that there will be continued warming over southwest Asia. The greatest warming trends are found over Pakistan. Severe temperature changes as portrayed by RCP 8.5 are likely to have severe effects on the environmental and atmospheric dynamics of the region. Increasing temperatures may increase the melting of ice in the northern parts of Pakistan, draining freshwater resources. Studies project a widespread retreat of glaciers and snow cover during the 21st century (Meehl et al. 2005; Meehl et al. 2006). Glacial retreat has been apparent since 1960s and it has intensified in the present decade (Yao et al. 2007). The increase of water flow in the rivers may in turn contribute to sea level rise (Zuo & Oerlemans 1997). Such changes are likely to result in a substantial impact on the climate and hydrology of the region.

Acknowledgments

This study acknowledges the support of the National Basic Research Program “973” of China (2012CB955200), and the Priority Academic Program Development of Jiangsu Higher Education Institutions (PAPD). Authors of this paper are thankful to the World Climate Research Program’s Working Group on Coupled Modeling, the U.S. Department of Energy's Program for Climate Model Diagnosis and Intercomparison and the Global Organization for Earth System Science Portals. We also appreciate the climate modeling groups (listed in Table 1 of this paper) for producing and making available their model output.

References

Arora, M., N. K. Goel & P. Singh, 2005: Evaluation of temperature trends over India / Evaluation de tendances de température en Inde. Hydrological Sciences Journal, 50(1), p.null-93.

Clarke, L. et al., 2007: Scenarios of greenhouse gas emissions and atmospheric concentrations. US Department of Energy Publications, p.6.

Cruz, R. V et al., 2007: Asia. In “Climate Change 2007: impacts, adaptation and vulnerability. Contribution of Working Group II to the Fourth Assessment Report of the Intergovernmental Panel on

Climate Change".(Eds ML Parry, OF Canziani, JP Palutikof, PJ van der Linden, CE Hanson. Cambridge, UK: Cambridge University Press. Accessed February, 28, p.2013.

Farooqi, A. B., A. H. Khan, & H. Mir, 2005: Climate change perspective in Pakistan. Pakistan J. Meteorol, 2(3).

Fujino, J. et al., 2006: Multi-gas mitigation analysis on stabilization scenarios using AIM global model. The Energy Journal, pp.343–353.

Hansen, J. E. et al., 2006: NASA GISS surface temperature (GISTEMP) analysis. Trends: A Compendium of Data on Global Change.

Hansen, J. et al., 2007: Climate simulations for 1880--2003 with GISS modelE. Climate Dynamics, 29(7–8), pp.661–696.

Harris, I. et al., 2014: Updated high-resolution grids of monthly climatic observations--the CRU TS3. 10 Dataset. International Journal of Climatology, 34(3), pp.623–642.

Hijioka, Y. et al., 2008: Global GHG emission scenarios under GHG concentration stabilization targets. Journal of Global Environment Engineering, 13, pp.97–108.

Hu, Z. et al., 2014: Temperature changes in Central Asia from 1979 to 2011 based on multiple datasets.

Imran, A. et al., 2014: An Analytical Study of the Variations in the Monsoon Patterns over Pakistan. Pakistan Journal of Meteorology Vol, 10(20).

IPCC, 2001: The Scientific Basis. Intergovernmental Panel on Climate Change. by JT Houghton, Y. Ding, DJ Griggs, et al.

IPCC, 2007: Climate change 2007-the physical science basis: Working group I contribution to the fourth assessment report of the IPCC, Cambridge University Press.

IPCC, 2013: Working Group I Contribution to the IPCC Fifth Assessment Report, Climate Change 2013: The Physical Science Basis. Ipcc, AR5 (March 2013), p.2014.

Johannessen, O. M. et al., 2004: Arctic climate change: Observed and modelled temperature and sea-ice variability. Tellus, Series A: Dynamic Meteorology and Oceanography, 56(4), pp.328–341.

Jones, P. D. & T. M. L. Wigley, 2010: Estimation of global temperature trends: What's important and what isn't. Climatic Change, 100(1), pp.59–69.

Karl, T. R., R.W. Knight, & J. R. Christy, 1994: Global and hemispheric temperature trends: Uncertainties related to inadequate spatial sampling. Journal of Climate, 7(7), pp.1144–1163.

Kim, H.-M., P. J. Webster, & J. A. Curry, 2012: Evaluation of short-term climate change prediction in multi-model CMIP5 decadal hindcasts. Geophysical Research Letters, 39(10).

Kumar, S. et al., 2013: Multidecadal climate variability and the "warming hole" in North America: Results from CMIP5 twentieth- and twenty-first-century climate simulations. Journal of Climate, 26(11), pp.3511–3527.

Lal, M. et al., 2001: Future climate change: Implications for Indian summer monsoon and its variability. Current science, 81(9), pp.1196–1207.

Meehl, G. A. et al., 2005: How much more global warming and sea level rise? Science, 307(5716), pp.1769–1772.

Meehl, G. A. et al., 2006: Climate change projections for the twenty-first century and climate change commitment in the CCSM3. Journal of climate, 19(11), pp.2597–2616.

Overland, J. E. et al., 2004: Seasonal and regional variation of pan-arctic surface air temperature over the instrumental record*. Journal of Climate, 17(17), pp.3263–3282.

Pant, G. B. & K. R. Kumar, 1997: Climates of south Asia, John Wiley & Sons.

Riahi, K., A. Grübler, & N. Nakicenovic, 2007: Scenarios of long-term socio-economic and environmental development under climate stabilization. Technological Forecasting and Social Change, 74(7), pp.887–935.

Sarker, R. P. & V. Thapliyal, 1988: Climate change and variability. Mausam, 39, pp.127–138.

Serreze, M. C. & J. A. Francis, 2006: The Arctic amplification debate. Climatic change, 76(3–4), pp.241–264.

Srivastava, H. N. et al., 1992: Decadal trends in climate over India. Mausam, 43(1), pp.7–20.

Stott, P. A. et al., 1998: Scale-Dependent Detection of Climate Change. Journal of Climate, 11(12), pp.3282–3294.

Stott, P. A. et al., 2000: External control of 20th century temperature by natural and anthropogenic forcings. Science, 290(5499), pp.2133–2137.

Taylor, K. E. et al., 2012: An Overview of CMIP5 and the Experiment Design. Bulletin of the American Meteorological Society, 93(4), pp.485–498.

Taylor, K. E., 2001: Summarizing multiple aspects of model performance in a single diagram. Journal of Geophysical Research: Atmospheres, 106(D7), pp.7183–7192.

Trenberth, K. E. et al., 2007: Observations: Surface and Atmospheric Climate Change Coordinating Lead Authors: Lead Authors: Executive Summary. Climate Change.

Van Vuuren, D. P. et al., 2007: Stabilizing greenhouse gas concentrations at low levels: an assessment of reduction strategies and costs. Climatic Change, 81(2), pp.119–159.

Willmott, C. J. & S. M. Robeson, 1995: Climatologically aided interpolation (CAI) of terrestrial air temperature. International Journal of Climatology, 15(2), pp.221–229.

Wise, M. et al., 2009: Implications of limiting CO2 concentrations for land use and energy. Science, 324(5931), pp.1183–1186.

Wu, Q., & D. J. Karoly, 2007: Implications of changes in the atmospheric circulation on the detection of regional surface air temperature trends. Geophysical research letters, 34(8).

Wu, Q., & D. M. Straus, 2004: AO, COWL, and observed climate trends. Journal of Climate, 17(11), pp.2139–2156.

Wu, Q., 2010: Associations of diurnal temperature range change with the leading climate variability modes during the Northern Hemisphere wintertime and their implication on the detection of regional climate trends. Journal of Geophysical Research: Atmospheres, 115(D19).

Yao, T. et al., 2007: Recent Glacial Retreat and Its Impact on Hydrological Processes on the Tibetan Plateau, China, and Surrounding Regions. Arctic, Antarctic, and Alpine Research, 39(4), pp.642–650.

Yu, R., B. Wang, & T. Zhou, 2004: Climate effects of the deep continental stratus clouds generated by the Tibetan Plateau. Journal of Climate, 17(13), pp.2702–2713.

Zhou, T., & Z. Li, 2002: Simulation of the East Asian summer monsoon using a variable resolution atmospheric GCM. Climate Dynamics, 19(2), pp.167–180.

Zuo, Z., & J. Oerlemans, 1997: Contribution of glacier melt to sea-level rise since AD 1865: a regionally differentiated calculation. Climate Dynamics, 13(12), pp.835–845.